ADVANCED MATERIALS

In summary, we have successfully produced highly ordered arrays of single-crystalline antimony nanowires with diameters of 40 nm in porous anodic alumina membranes by pulsed electrodeposition. The results of XRD and HRTEM indicate that the nanowires have a uniform hexagonal antimony single-crystalline structure and grow along the [11$\bar{2}$0] direction. The resistance at zero magnetic field demonstrates that single-crystalline antimony nanowires with diameters of 40 nm remain metallic in character. It would be very interesting to produce a metal–semiconductor nanowire heterogeneous junction array consisting of antimony metal and bismuth semiconductor. Further work is under way.

Experimental

The AAM was prepared as follows: high purity (99.999 %) aluminum was electropolished at 23 V in a mixture solution of 70 % perchloric acid and ethanol (1:9) at 4 °C for 2 min. Anodization was carried out at 40 V DC in 0.25 M aqueous oxalic acid electrolyte at 7 °C. After the anodization, the central substrate was removed in a saturated $SnCl_4$ solution, and the surrounding aluminum was retained as a support. Then the barrier was dissolved in 6 wt.-% phosphoric acid solution at 30 °C for 60 min. Finally, a layer of Au was sputtered onto one side of the AAM to serve as the working electrode. Field-emission microscopy observations indicate that the AAM is an almost perfect hexagonally arranged nanochannel array with a channel diameter of ~ 40 nm.

The antimony plating solution consisted of 0.02 M $SbCl_3$, 0.1 M $C_6H_8O_7{\cdot}H_2O$, and 0.05 M $K_3C_6H_5O_7{\cdot}H_2O$. The initial pH was adjusted to 2 by adding appropriate amounts of 5 M H_2SO_4 solution. The pulsed electrodeposition was performed at 12 °C.

The antimony nanowire arrays were observed using a field emission microscope (JEOL JSM-6700F) and a transmission electron microscope (JEOL 200CX and JEL 2010). For TEM analysis, the specimens were prepared by dissolving the AAMs with 5 wt.-% NaOH solution, dispersing the antimony nanowires in ethanol by ultrasonic vibration, and then placing drops of the dispersion on carbon films on a copper grid. The FEM specimen was obtained by dissolving the upper part of the AAM with 5 wt.-% NaOH solution. The X-ray diffraction spectrum was obtained using a rotating anode X-ray diffractometer (D/MAX-rA) with Cu Kα radiation ($\lambda = 1.542$ Å). The electrical resistance was measured by the standard DC four-probe method in the temperature range from 20 K to 273 K.

Received: May 16, 2002
Final version: June 12, 2002

[1] M. Saito, M. Kirihara, T. Taniguchi, M. Miyagi, *Appl. Phys. Lett.* **1989**, *55*, 607.
[2] S. Iijima, *Nature* **1991**, *354*, 56.
[3] R. J. Tonucci, B. L. Justus, A. J. Campillo, C. E. Ford, *Science* **1992**, *258*, 783.
[4] H. Dai, E. W. Wong, Y. Z. Lu, S. Fan, C. M. Lieber, *Nature* **1995**, *375*, 769.
[5] A. M. Morales, C. M. Lieber, *Science* **1998**, *279*, 208.
[6] S. J. Tans, R. M. Verschueren, C. Dekker, *Nature* **1998**, *393*, 49.
[7] X. F. Duan, Y. Huang, Y. Cui, J. F. Wang, C. M. Lieber, *Nature* **2001**, *409*, 66.
[8] J. D. Klein, R. D. Herrick, D. Palmer, M. J. Sailor, C. J. Brumlik, C. R. Martin, *Chem. Mater.* **1993**, *5*, 902.
[9] C. K. Preston, M. Moskovits, *J. Phys. Chem.* **1993**, *97*, 8495.
[10] C. A. Huber, T. E. Huber, M. Sadoqi, J. A. Lubin, S. Manolis, C. B. Prater, *Science* **1994**, *263*, 800.
[11] G. Sauer, G. Brehm, S. Schneider, K. Nielsch, R. B. Wehrspohn, J. Choi, H. Hofmeister, U. Gösele, *J. Appl. Phys.* **2002**, *91*, 3243.
[12] D. Routkevitch, T. Bigioni, M. Moskovits, J. M. Xu, *J. Phys. Chem.* **1996**, *100*, 14 037.
[13] X. Y. Zhang, L. D. Zhang, G. W. Meng, G. H. Li, N. Y. Jin-Phillipp, F. Phillipp, *Adv. Mater.* **2001**, *13*, 1238.
[14] H. Q. Cao, Y. Xu, J. M. Hong, H. B. Liu, G. Yin, B. L. Li, C. Y. Tie, Z. Xu, *Adv. Mater.* **2001**, *13*, 1393.
[15] M. S. Sander, A. L. Prieto, R. Gronsky, T. Sands, A. M. Stacy, *Adv. Mater.* **2002**, *14*, 665.
[16] G. L. Che, B. B. Lakshmi, E. R. Fisher, C. R. Martin, *Nature* **1998**, *393*, 346.
[17] J. Li, C. Paradopoulos, J. M. Xu, *Appl. Phys. Lett.* **1999**, *75*, 367.
[18] R. Parthasarathy, C. R. Martin, *Nature* **1994**, *369*, 298.
[19] L. R. Windmiller, *Phys. Rev.* **1966**, *149*, 472.
[20] Z. Zhang, J. Y. Ying, M. S. Dresselhaus, *J. Mater. Res.* **1998**, *13*, 1754.
[21] J. Heremans, C. M. Thrush, Y. M. Lin, S. Cronin, Z. Zhang, M. S. Dresselhaus, J. F. Mansfield, *Phys. Rev. B* **2000**, *61*, 2921.
[22] A. L. Prieto, M. S. Sander, M. S. Martin-González, R. Gronsky, T. Sands, A. M. Stacy, *J. Am. Chem. Soc.* **2001**, *123*, 7160.
[23] M. Barati, J. C. L. Chow, P. K. Ummat, W. R. Datars, *J. Phys.: Condens. Matter* **2001**, *13*, 2955.
[24] J. Heremans, C. M. Thrush, Y. M. Lin, S. B. Cronin, M. S. Dresselhaus, *Phys. Rev. B* **2001**, *63*, 85 406.
[25] D. Dobrev, J. Vetter, N. Angert, R. Neumann, *Appl. Phys. A* **1999**, *69*, 233.
[26] D. Dobrev, J. Vetter, N. Angert, R. Neumann, *Appl. Phys. A* **2001**, *72*, 729.
[27] K. H. Choi, H. S. Kim, T. H. Lee, *J. Power Sources* **1998**, *75*, 230.
[28] K. Nielsch, F. Müller, A. P. Li, U. Gösele, *Adv. Mater.* **2000**, *12*, 582.
[29] M. Sun, G. Zangari, M. Shamsuzzoha, R. M. Metzger, *Appl. Phys. Lett.* **2001**, *78*, 2964.
[30] International Centre for Diffraction Data (ICDD), Newtown Square, PA, Powder Diffraction File, formerly JCPDS.

Spin-Driven Resistance in Organic-Based Magnetic Semiconductor V[TCNE]$_x$**

By *Vladimir N. Prigodin*, *Nandyala P. Raju*, *Konstantin I. Pokhodnya*, *Joel S. Miller*, and *Arthur J. Epstein**

In the past decade there has been extensive progress in using the spin property of electrons in inorganic multilayers as a means of introducing revolutionary new types of electronics (e.g., spin valves, spin light-emitting diodes) termed spintronics.[1] Challenges including improved spin injection through interfaces between different materials, sensitivity to weak magnetic fields, as well as low Curie temperatures remain.[2] We report that these challenges may be overcome with polymers due to the flexibility of polymer/molecular chemistry. The conductivity of conjugated polymers is readily controlled between insulators and metals (over 15 decades) by doping and structural order.[3] Similarly bright electroluminescence has been achieved in polymer and molecular films.[4] Organic-based magnets started with discovery[5] in the mid 1980s of ferromagnetism below an ordering temperature of 4.8 K in the linear chain electron transfer salt [$FeCp^*_2$]-[TCNE] ([TCNE] = tetracyanoethylene (Fig. 1a; C_p^* = pentamethylcyclopentadienide). Among the many organic-based magnets subsequently reported, vanadium-tetracyanoethylene (V[TCNE]$_x$, $x \sim 2$) is a "soft" ferrimagnet with ordering temperature $T_c \sim 400$ K, a small coercive field $H_c = 4.5$ G at 300 K, and room temperature (RT) semiconducting conductivity $\sigma_{RT} \sim 10^{-4}$ S cm^{-1}. It can be prepared at 40 °C using chemical vapor deposition (CVD).[6]

[*] Prof. A. J. Epstein, Prof. V. N. Prigodin, Dr. N. P. Raju, Prof. K. I. Pokhodnya
Department of Physics, The Ohio State University
Columbus, OH 43210-1106 (USA)
E-mail: Epstein@mps.ohio-state.edu
Prof. J. S. Miller
Department of Chemistry, University of Utah
Salt Lake City, UT 84112-0850 (USA)

[**] Supported in part by the Department of Energy Grant Nos. DE-FG02-01ER45931 and DE FG 03-93ER45504, and the Army Research Office Grant No. F49620-00-0055.

  0935-9648/02/1709-1230 $ 17.50+.50/0

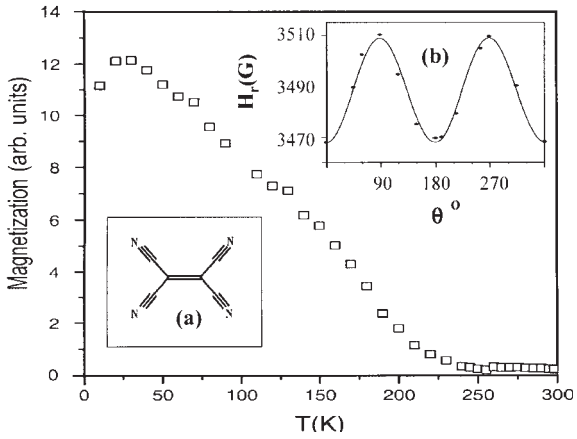

Fig. 1. Magnetization of a V[TCNE]$_x$ film vs. temperature for magnetic field $H = 6$ kG directed perpendicular to film. Insets: a) Chemical structure of TCNE. b) Anisotropy of EPR resonance field H_r at $T = 100$ K.

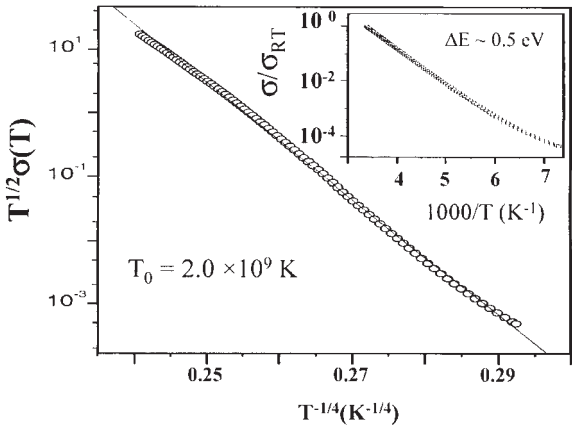

Fig. 2. Conductivity of V[TCNE]$_x$ film plotted as $T^{1/2}\sigma(T)$ vs. $T^{-1/4}$ (3D VRH). Inset: fit of $\sigma(T)$ to the activated (Ahrrenius) behavior. An energy gap of 0.5 eV is obtained.

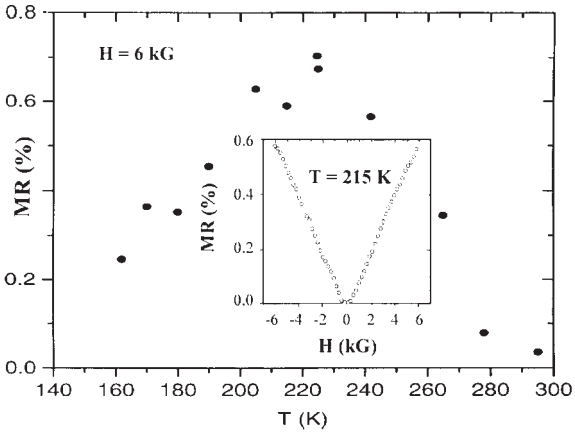

Fig. 3. Temperature dependence of magnetoresistance in V[TCNE]$_x$ film for plane of the film parallel to the applied field $H = 6$ kG for the sample of Figure 1. Inset: $MR(H)$ for $T = 215$ K.

Here, we present magnetotransport studies of films of V[TCNE]$_x$ to evaluate its potential applicability for spintronic applications as a source or an analyzer of spin polarized charge current.[1] We report the first observation of an increase in resistance with applied magnetic field (positive magnetoresistance) for V[TCNE]$_x$ (x ~ 2) at room temperature, up to ~0.7 % at $H = 6$ kG. Squeezing of electron wave functions by magnetic field (a mechanism for the positive magnetoresistance in conventional disordered semiconductors) predicts a magnetoresistance three orders of magnitude less than the observed value. We have shown that the observed anomalous value of magnetoresistance in V[TCNE]$_x$ and its variations with magnetic field and temperature are consistent with spin polarized charge transport.

The samples fabricated as solvent-free CVD prepared thin films were characterized magnetically with electron paramagnetic resonance (EPR). Figure 1 shows the magnetization (a result of integrating the EPR signal) of a film vs temperature. Study of the lower T_c sample (T_c ~ 230 K here) enables us to probe magnetotransport above and below T_c. Below T_c there is anisotropy in the resonance magnetic field (Fig. 1b) due to the dependence of the demagnetization factor on the orientation of magnetic field to the film.

Figure 2 shows the DC-conductivity as function of temperature. There is a fit to Mott's 3D variable range hopping (VRH) for localized charge carriers[7] $\sigma_{DC} \sim T^{-1/2} \exp[-(T_0/T)^{1/4}]$ with $T_0 = 2.0 \times 10^9$ K. Here, $T_0 = B/[N(\varepsilon_F)\xi^3]$, where $B = 21.2$, $N(\varepsilon_F)$ is the density of states at the Fermi level, and ξ is the localization radius. Assuming ξ ~ 0.5 nm (length of TCNE), we find $N(\varepsilon_F) \sim 1.0 \times 10^{18}$ (eV)$^{-1}$ cm^{-3} too low for the charge density obtained from space filling arguments $n \sim 1/(0.5\text{ nm})^3 \sim 10^{22}$ cm^{-3}. Therefore, we replot the $\sigma(T)$ for a simple activation dependence with energy gap ΔE ~ 0.5 eV (inset, Fig. 2).

Figure 3 shows the temperature dependence of magnetoresistance $MR = [\rho(H,T)-\rho(0,T)]/\rho(0,T)$ of V[TCNE]$_x$ sample with T_c ~ 230 K derived from $M(T)$ (Fig. 1). The applied magnetic field $H = 6$ kG is parallel to the film. The same MR is observed for the magnetic field perpendicular to the film. The maximum of $MR(T)$ is below but close to T_c. The inset in Figure 3 illustrates the H-dependence of MR for $T = 215$ K and magnetic field parallel to the film. Similar linear field dependence was obtained for all temperatures below T_c and samples with different T_c. Figure 4 illustrates $MR(T)$ of a sample with a higher $T_c \sim 280$ K. The maximum of $MR(T)$ clearly correlates with the magnetic ordering temperature as shown in the inset of Figure 4.

It is conventional for a semiconductor with $\rho(T) = \rho_0 \exp[(T_0/T)^{1/4}]$ to account for the positive MR as being due to squeezing of localized wave functions in the presence of magnetic field. For a weak magnetic field the theory yields:[7] $\ln[\rho(H,T)/\rho(0,T)] = A(\xi/\lambda)^4(T_0/T)^{3/4}$, where $A = 5/2016$ and λ is the magnetic length: $\lambda = (c\hbar/eH)^{1/2}$. The regime of weak magnetic field is valid so long as $\lambda \gg \xi$. For V[TCNE]$_x$ the localization length $\xi \sim 0.5$ nm, $\lambda = 33.1$ nm for $H = 6$ kG, and experimentally $T_0 = 2.0 \times 10^9$ K. For $T = 215$ K and $H = 6$ kG we find $[\rho(H,T)-\rho(0,T)/\rho(0,T)] = 3.6 \times 10^{-6}$, i.e., the MR is very small. (We tested this conclusion using the non-magnetic semiconducting polymer with similar hopping transport, sulfonated

  0935-9648/02/1709-1231 $ 17.50+.50/0

ADVANCED MATERIALS

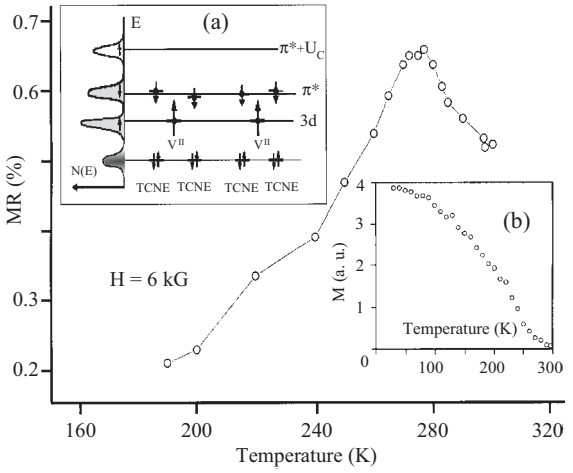

Fig. 4. $MR(T)$ for V[TCNE]$_x$ (x ~ 2) sample with T_c ~280 K derived from magnetization (M, inset b). Inset a): Schematic of level diagram for V[TCNE]$_2$. Half-filled π*-band of [TCNE]$^-$ is split into two non-overlapping subbands by the strong Coulomb repulsion U_c.

polyaniline;[8] and no MR was detected at these temperatures.) Thus, the observed $MR \sim 6 \times 10^{-3}$ in V[TCNE]$_x$ is larger than that for conventional semiconductors by three orders of magnitude. Also the experimental H- and T-dependencies of MR are not consistent with the conventional model.

To explain the anomalous MR we consider the electronic structure and the origin of magnetic order in V[TCNE]$_x$. From an average stoichiometry and the magnetic saturation moment, it is assumed[9] that $S = 3/2$ V^{II} has its unpaired electrons in 3d orbitals and $S = 1/2$ $[TCNE]^{\bullet -}$ has its unpaired electron in its π* orbital. Figure 4a depicts the 1D spatial distribution of energy levels in V[TCNE]$_2$. V^{II} is shown alternating with two $[TCNE]^-$ ions to reflect the nominal stoichiometry. The orientation of electronic spins in the π*-state is opposite (antiferromagnetic) to the 3/2-spin of V^{II} and the net magnetic spin of the V^{II}-complex with $[TCNE]^{\bullet -}$ ligands is 1/2.

The charge transport involves hopping among $[TCNE]^{\bullet -}$s. The LUMO π* orbital of each $[TCNE]^{\bullet -}$ can accept two electrons with opposite spins, but the energy of this double occupied $[TCNE]^{2-}$ includes the additional Coulomb repulsion U_c. In analogy with known organic materials and from the activation energy of conductivity the effective U_c is ~ 0.5 eV. The relevant model for description of electronic states on $[TCNE]^{\bullet -}$ is the Hubbard model with nearly half-filling.[10] Here, the π* band is spilt into two non-overlapping subbands provided $U_c \gg t$, where t is the electronic transfer-integral between neighboring $[TCNE]^{\bullet -}$s. The spins of electrons in the lower filled Hubbard subband should have antiferromagnetic order but the corresponding exchange constant $J' = 2t^2/U_c$ is much less than J. Therefore, in the magnetic phase the electronic spins of lower subband are parallel and their orientation is opposite to the spin of V^{II}. According to the Pauli exclusion principle, the upper empty subband may be occupied by electrons with spins polarized in the direction opposite to the lower subband, i.e., parallel to the orientation of V^{II} spins.

For the nearly stoichiometric case the temperature dependence of the conductivity is determined by thermal activation across the energy gap: $\sigma(T) = e\mu n_a(T)$, where n_a is the concentration of carriers in the upper conduction π* subband and μ is their mobility. The total concentration of π* electrons V^{II} is $n \sim 10^{22}$ cm^{-3} and $n_a \sim n\exp[-\Delta E/(k_B T)] \sim 10^{15}$ cm^{-3} for $\Delta E = U_c \sim 0.5$ eV and $T = 300$ K. This value n_a implies a RT mobility in V[TCNE]$_x$ with $\sigma_{RT} \sim 10^{-4}$ S cm^{-1} to be the same as in amorphous Si, $\mu \sim 0.1$ cm^2/(V s).

Applying the magnetic field changes the mobility by modulation of hopping rates, but a stronger field effect on the conductivity is through the change of activation gap. Taking into account the opposite spin polarizations of π* subbands and their antiferromagnetic coupling with V^{II} spins, the energy gap ΔE is approximated as $\Delta E = U_c - 4J\langle S\rangle\langle\sigma\rangle$, where $\langle S\rangle$ is the spin 3/2 polarization of V^{II} and $\langle\sigma\rangle$ is the spin 1/2 polarization of lower π* subband. In the paramagnetic phase the spin polarizations are induced by an external magnetic field and become noticeable only upon approaching T_c. Within the mean field theory[11] $\langle S\rangle \sim -\langle\sigma\rangle \sim \chi h$, where χ is the Curie-Weiss susceptibility per spin, $\chi \sim 1/\delta$, with $\delta = (T - T_c)/T_c$ being the "distance" from T_c ($k_B T_c \sim 3.2$ J). Here, $h = \mu_B g H/(k_B T_c) \ll 1$ and $h^{2/3} \ll \delta \ll 1$. As a result the gap widens with the applied field and $MR \sim (h/\delta)^2$. In the critical region, $|\delta| \ll h^{2/3}$, the induced polarization obeys the scaling law $\langle S\rangle \sim -\langle\sigma\rangle \sim h^{1/3}$ and $MR \sim h^{2/3}$. Below T_c ($|\delta| \gg h^{2/3}$, $\delta < 0$), there is the spontaneous spin polarization $\langle S\rangle \sim -\langle\sigma\rangle \sim |\delta|^{1/2}$ with field dependent corrections ~ χh, where $\chi \sim 1/|\delta|$. Therefore, in the ferrimagnetic phase the MR is proportional to a magnetic field and decreases far below T_c, $MR \sim h/|\delta|^{1/2}$.

As a function of temperature, the MR has the maximum near T_c. For $H = 6$ kG and $T_c = 230$ K the model predicts the MR maximum ~ $h^{2/3} \sim 2$ %, which is of the order of the observed value. The model also reproduces the experimental linear field dependence of MR below T_c (inset, Fig. 3). Figures 3 and 4 indicate that the position of maximum of $MR(T)$ and T_c are correlated. A random magnetic anisotropy arising from strain and composition inhomogeneities leads to glassy behavior[12] and may shift the maximum in $MR(T)$ and $\chi(T)$ below T_c.

Thus, the experimental results for resistance and MR of organic-based magnet V[TCNE]$_x$ support the existence of spin polarized subbands—a half semiconducting state—in which the electron spins in "valence and conduction bands" are oppositely polarized. This is a very desirable property for utilizing organic-based magnetic semiconductors in spintronic applications.

Received: April 25, 2002
Final version: June 6, 2002

[1] S. A. Wolf, *J. Supercond.* **2000**, *13*, 195.
[2] H. Ohno, F. Matsukura, *Solid State Commun.* **2001**, *117*, 179.
[3] R. S. Kohlman, A. J. Epstein, in *Handbook of Conducting Polymers* (Eds: T. A. Skotheim, R. L. Elsenbaumer, J. R. Reynolds), Marcel Dekker Inc., New York **1998**, p. 85.
[4] See, for example, CDT website: www.cdtltd.co.uk.
[5] J. S. Miller, J. C. Calabrese, A. J. Epstein, R. W. Bigelow, J. H. Zhang, W. M. Reiff, *J. Chem. Soc., Chem. Commun.* **1986**, 1026.
[6] K. I. Pokhodnya, A. J. Epstein, J. S. Miller, *Adv. Mater.* **2000**, *12*, 410.
[7] B. I. Shklovskii, A. L. Efros, *Electronic Properties of Doped Semiconductors*, Springer-Verlag, Berlin **1984**, p. 155.

  0935-9648/02/1709-1232 $ 17.50+.50/0

[8] W. P. Lee, K. R. Breneman, A. D. Gudmundsdottir, M. S. Platz, P. K. Kahol, A. P. Monkman, A. J. Epstein, *Synth. Met.* **1999**, *101*, 819.
[9] J. S. Miller, A. J. Epstein, *Chem. Commun*. **1998**, 1319.
[10] S. Onoda, M. Imada, *J. Phys. Soc. Jpn.* **2001**, *70*, 3398.
[11] J. M. Yeomans, *Statistical Mechanics of Phase Transitions*, Oxford Univ. Press, New York **1992**, p. 128.
[12] a) P. Zhou, B. G. Morin, J. S. Miller, A. J. Epstein, *Phys. Rev. B* **1993**, *48*, 1325. b) K. I. Pokhodnya, D. Pejakovic, A. J. Epstein, J. S. Miller, *Phys. Rev. B* **2001**, *63*, 174 408.

Cyclopalladated Complexes as Photorefractive Materials with High Refractive Index Modulation**

By *Iolinda Aiello, Davide Dattilo, Mauro Ghedini, Andrea Bruno, Roberto Termine,* and *Attilio Golemme**

The development of organic materials for optoelectronic and photonic applications is the subject of intense research efforts, propelled by the ease of processability and of chemical modification and by the low cost of amorphous organic substances. Media in which information can be encoded by using light are of particular interest and among these novel organic materials with photorefractive properties[1–4] have attracted a remarkable interest during the last decade. A vast number of different classes of organic photorefractive materials are known, including polymers,[5–8] other glasses,[9–11] and liquid crystals.[12–17] In photorefractive substances the refractive index can be modulated by electric fields deriving from the space redistribution of photogenerated mobile charges: both photoconductivity and a field dependent refractive index are then necessary requirements.[18] In organic photorefractive materials, the different functions associated with the photogeneration, the transport, and the trapping of charges and with the field induced refractive index variation are usually provided by different molecules, in a solid solution or chemically linked within a polymeric structure. This reduces the relative concentration and the performance of each molecular species. In this paper, we present the excellent photorefractive properties of cyclopalladated complexes, a class of materials which exhibit both photoconductivity and field dependent refractive index.

In Figure 1 we show the molecular structure of the two cyclopalladated complexes AZPON and BEPON, synthesized as described elsewhere.[19] It was already shown that in AZPON it is possible to obtain photogenerated gratings which are phase shifted with respect to the original light interference pattern.[20] We will show below how BEPON, which is a compound of the same chemical class, also exhibits high photorefractive performance, which can then be considered as a property of the whole chemical class and not something due to the specific nature of a single molecule. Both substances are in a stable crystalline state at room temperature (RT), but BEPON shows a considerable tendency to undercool to an amorphous state with a glass transition temperature T_g ~ 24 °C. At RT BEPON can remain in an amorphous state for weeks, long enough to perform characterizations of its photorefractive properties. To obtain an amorphous phase containing AZPON, it was instead necessary to mix it with inert polymers, such as polystyrene (PS) or polyisobutylmethacrylate (PIBM).

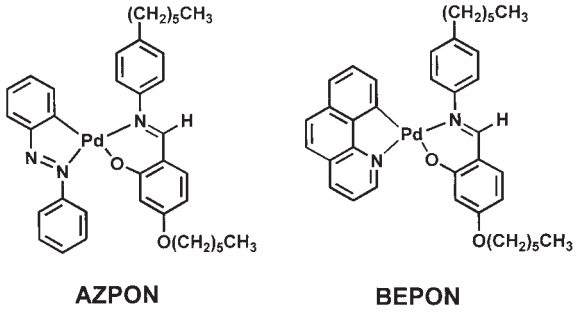

Fig. 1. Molecular structure of AZPON and BEPON. These complexes contain a palladium(II) center bonded in a square planar geometry.

Holographic characterizations of photorefractive materials are typically carried out by measuring the diffraction efficiency η in four-wave mixing experiments. The efficiency depends mainly on the amplitude Δn of the refractive index modulation induced by the space-charge field. In Figure 2a

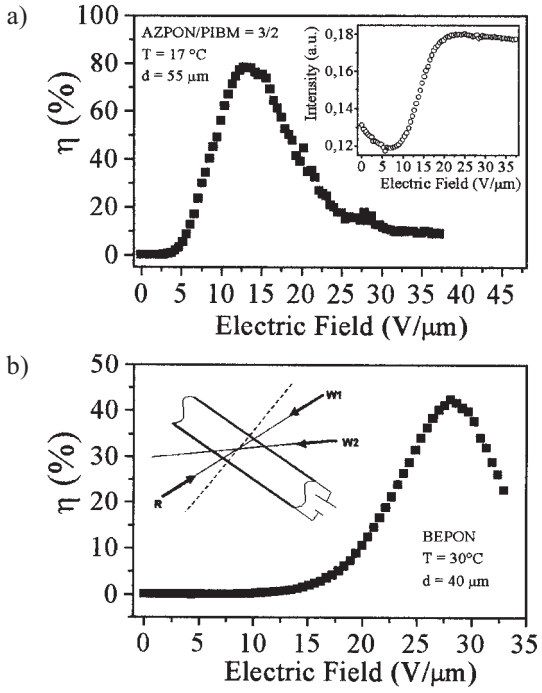

Fig. 2. a,b) Diffraction efficiency for AZPON/PIBM = 3/2 and BEPON as a function of the applied field. The measurements were performed at $\lambda = 633$ nm and with a grating period Λ ~3 μm. The inset in (a) shows the field dependence of the transmitted intensity of the reading beam when no writing beams, and no grating, are present. The inset in (b) shows the relative orientation of sample normal (dashed line), writing beams (W1 and W2) and reading beam (R).

[*] Prof. A. Golemme, Dr. I. Aiello, Dr. D. Dattilo, Prof. M. Ghedini, Dr. A. Bruno, Dr. R. Termine
Laboratory for the Synthesis, Characterisation and Applications of Molecular Materials (LASCAMM)
Dipartimento di Chimica, Università della Calabria
I-87030 Rende (Italy)
E-mail: a.golemme@unical.it

[**] This work was supported by CIPE grants (Clusters 14 and 26) from MURST.

  0935-9648/02/1709-1233 $ 17.50+.50/0